Talanta 85 (2011) 1680–1688

Contents lists available at ScienceDirect

Talanta

journal homepage: www.elsevier.com/locate/talanta

Rationally designed molecularly imprinted polymers for selective extraction of methocarbamol from human plasma

Mohammad Bagher Gholivand*, Mehdi Khodadadian

Department of Analytical Chemistry, Faculty of Chemistry, Razi University, Kermanshah, Iran

ARTICLE INFO

Article history:
Received 10 January 2011
Received in revised form 26 May 2011
Accepted 27 June 2011
Available online 2 July 2011

Keywords:
Molecularly imprinted polymer (MIP)
Methocarbamol
Density functional theory (DFT)
Solid-phase extraction (SPE)
Differential pulse voltammetry (DPV)

ABSTRACT

Molecularly imprinted polymers (MIPs) with high selectivity toward methocarbamol have been computationally designed and synthesized based on the general non-covalent molecular imprinting approach. A virtual library consisting of 18 functional monomers was built and possible interactions between the template and functional monomers were investigated using a semiempirical approach. The monomers with the highest binding scores were then considered for additional calculations using a more accurate quantum mechanical (QM) calculation exploiting the density functional theory (DFT) at B3LYP/6-31G(d,p) level. The cosmo polarizable continuum model (CPCM) was also used to simulate the polymerization solvent. On the basis of computational results, acrylic acid (AA) and tetrahydrofuran (THF) were found to be the best choices of functional monomer and polymerization solvent, respectively. MIPs were then synthesized by the precipitation polymerization method and used as selective adsorbents to develop a molecularly imprinted solid-phase extraction (MISPE) procedure before quantitative analysis. After MISPE the drug could be determined either by differential pulse voltammetry (DPV), on a glassy carbon electrode modified with multiwalled-carbon nanotubes (GC/MWNT), or high performance chromatography (HPLC) with UV detection. A comparative study between MISPE-DPV and MISPE-HPLC-UV was performed. The MISPE-DPV was more sensitive but both techniques showed similar accuracy and precision.

1. Introduction

Methocarbamol (Scheme 1), a carbamate structural analogue of the aryl glycerol ethers, is a centrally active muscle relaxant and widely used for the treatment of skeletal muscle conditions of pain and discomfort [1,2]. Methocarbamol is easily absorbed from the intestine and widely distributed in all body tissues [3]. Because of potential for severe side effects, this drug is on the list for high risk medications in the elderly [4].

The sensitive and fast monitoring of methocarbamol in body fluids is of great interest from both pharmacokinetic and forensic aspects [4–6]. The determination of methocarbamol in biological fluids is usually carried out by chromatographic techniques [6–9]. Compared to chromatography, voltammetric techniques have several advantages such as their low cost, sensitivity and short analysis time. However, one of the drawbacks of conventional voltammetric techniques is their low selectivity for target molecules in complex matrices such as biological samples [10]. To overcome this problem, a clean-up procedure such as liquid–liquid extraction (LLE) or solid-phase extraction (SPE) should be applied to reduce matrix complexity prior to quantitative analysis. In the past, LLE has played a major role in sample clean-up and preconcentration of the sample components to be measured. However, recovery of sample components by liquid extraction is seldom complete. Liquid extraction tends to be slow and labor-intensive. Additionally, more stringent environmental concerns are making the use and disposal of large amounts of organic solvents more difficult. On the other hand, the popularity and use of SPE are growing at a fast rate. SPE is easily automated, faster, and in general more efficient than LLE. However, the selectivity of commercial SPE sorbents is low and this makes a problem when a selective extraction from a complex matrix has to be performed.

To enhance the molecular selectivity in SPE, molecularly imprinted polymers have been developed [11–15]. MIPs are cross-linked macromolecules bearing “tailor-made” binding sites for target molecules. They are prepared by the complexation, in solution, of a target compound (template) with functional monomers, through either covalent or non-covalent bonds, followed by polymerization with an excess of cross-linker to form a highly cross-linked polymer network. Upon removal of the template molecule from the polymer network, specific recognition sites that are complementary to the template in terms of their size, shape, and functionality are exposed [16,17]. As a result of their chemical and physical robustness, in combination with the

* Corresponding author. Tel.: +98 831 4274557; fax: +98 831 4274559.
E-mail address: mbgholivand@yahoo.com (M.B. Gholivand).

0039-9140/$ – see front matter © 2011 Elsevier B.V. All rights reserved.
doi:10.1016/j.talanta.2011.06.066

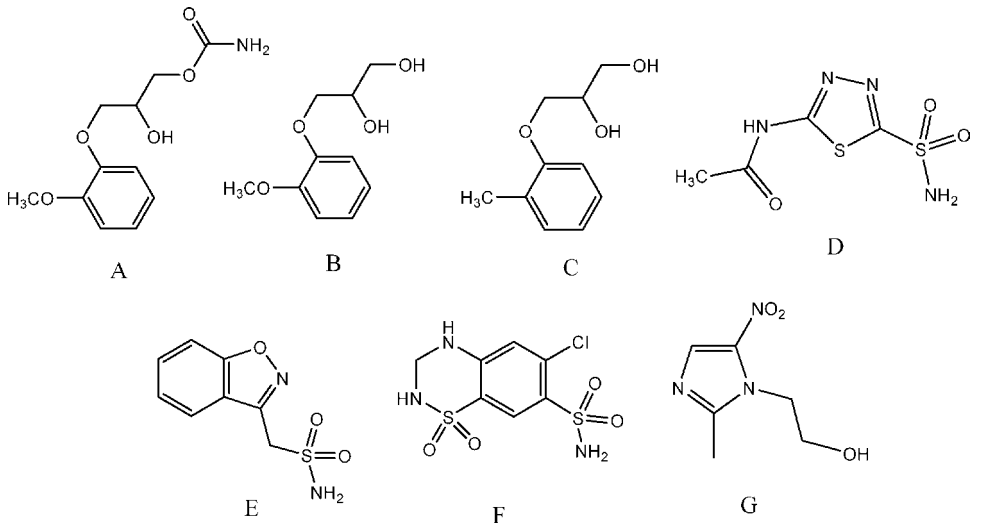

Scheme 1. Chemical structures of: (a) methocarbamol, (b) guaifenesin, (c) mephenesin, (d) acetazolamide, (e) zonisamide, (f) hydrochlorothiazide and (g) metronidazole.

polymer's selectivity, MIPs have proven to be good adsorbents for MISPE applications [18,19]. Nevertheless, general molecular imprinting protocols are tedious and time-consuming because they are based on trial and error method to find the best conditions for imprinting process.

Recently the combinatorial and computational methods have been considered as alternative approaches for the rational design of MIPs [20–22]. The characterization of molecular complexes formed between templates and monomers, with the aim of achieving a clearer picture of the interactions that are the basis of MIP technology, has been the goal of numerous theoretical studies [23]. Over the past few years, a number of studies have been reported describing the application of *ab initio* and DFT computational methods in the rational design of MIPs [21,24,25]. However, the long computation times required for geometry optimization is one of the drawbacks of such calculations. One way of reducing computation time, however, is to combine the fast computational methods such as molecular mechanics (MM) or semiempirical calculations with *ab initio* or DFT methods. For example, a large library of functional monomers can be screened fast by applying a semiempirical method followed by a DFT optimization on the most stable structures. This will reduce the computation time by the fast rejection of functional monomers which do not interact with the template molecule intensively.

Electroanalytical techniques have some important advantages including speed, high sensitivity, relative simplicity and low costs compared to other techniques. In recent years, the application of carbon nanotubes in electrode modification has received remarkable attention in electrochemistry [26–32]. The modification of electrode substrates with MWNTs would result in low detection limits, reduced overpotentials and resistance to surface fouling and therefore MWNTs have been claimed as electrocatalysts [26,28,29,32].

Herein, the semiempirical and DFT-quantum mechanical calculations were used for the rational design of methocarbamol-imprinted polymers. The MIPs were then synthesized to develop a MISPE procedure for the selective extraction of methocarbamol from human plasma before quantitative analysis by DPV or HPLC-UV.

2. Experimental

2.1. Materials

Methocarbamol (99.8%), mephenesin, guaifenesin, zonisamide, hydrochlorothiazide, metronidazole, acetazolamide and 4-vinylpyridine (4-VP) all were purchased from Sigma (Madrid, Spain). A standard solution of 100 $\mu g\,mL^{-1}$ of methocarbamol was prepared by dissolving an appropriate amount of the drug in methanol. This solution was stored at dark and 4 °C. Other diluted solutions were prepared by dilution from the standard solution. Acrylic acid (AA), ethylene glycol dimethacrylate (EGDMA), 2,2′-azobis(isobutyronitrile) (AIBN), triethylamine (TEA), trifluoroacetic acid (TFA) and HPLC grade solvents such as methanol (MeOH) and acetonitrile (MeCN) were purchased from Merck (Darmstadt, Germany). All monomers were distilled under the reduced pressure to remove their stabilizers before use. Human plasma samples were obtained from healthy volunteers and stored at −20 °C until use. All other chemical were of analytical reagent grade and used without further purification.

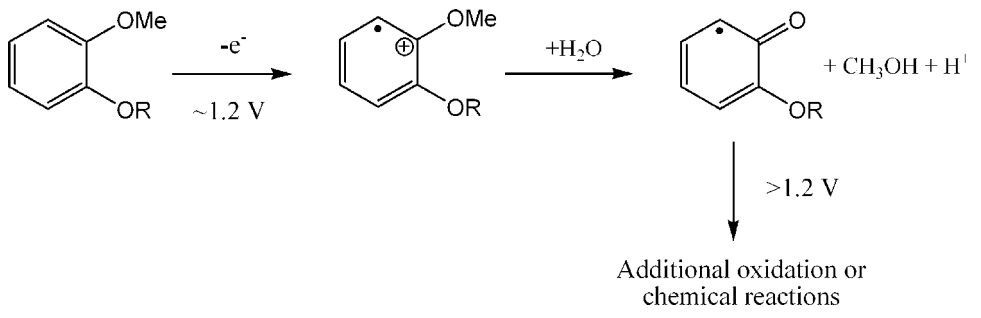

Scheme 2. Possible electrode reaction of methocarbamol.

2.2. Instrumentation

All voltammograms were recorded using an AUTOLAB instrument with GPES 4.9 software. Measurements were carried out on a GC or GC/MWNT electrode in a three-electrode arrangement. The auxiliary electrode was a wire of platinum; and an Ag/AgCl electrode was used as reference electrode. All measurements were carried out at room temperature. A Metrohm-780 pH-meter (Switzerland) was used for pH adjustments.

High performance liquid chromatography (HPLC) was performed on a CECIL liquid chromatograph instrument. The variable wavelength UV–visible detector was operated at 275 nm for methocarbamol determination. A 20 μL injection loop and a reversed phase C18 column (250 × 4.0 mm i.d., HICHROM, H50DS-13272) were used. The mobile phase was 50/50 (v/v) mixture of 0.02 mol L^{-1} phosphate buffer/acetonitrile adjusted to pH 3.0 at a flow rate of 1 mL min^{-1}. A Windaus two-channel peristaltic pump model D-38678 was used to pump solvents during MISPE experiments.

2.3. General procedure for recording voltammograms

The general procedure for obtaining voltammetric curves was as follows: 10.0 mL of 0.1 M phosphate buffer pH 3.0 was transferred into the voltammetric cell. After purging the solution with high purity nitrogen, the voltammogram was recorded as background curve over the potential range from 0.7 to 1.5 V using the DPV mode on a GC/MWNT electrode. The required aliquot of the standard solution of methocarbamol was added by means of a micropipette and its voltammogram was recorded as before. The pulse amplitude of 100 mV, pulse width of 250 ms and a scan rate of 100 mV s^{-1} were used for differential pulse voltammetry. All of the electrochemical experiments were carried out at ambient laboratory temperature (25 °C). Between experiments, the cell was treated with concentrated nitric acid and then washed with double distilled water.

2.4. Preparation of the GC/MWNT electrode

The bare GC electrode was polished successively with 1 and 0.05 μm alumina slurries to a mirror surface, and cleaned in ethanol and water under ultrasonication. A droplet (5 μL) DMF suspension of the MWNTs (0.5 mg mL^{-1}) was spread on the disk surface of the GC electrode using a micro-syringe. Than the electrode was dried in the air forming the MWNT modified GC electrode, denoted as the GC/MWNT.

2.5. Synthesis of polymers

General procedure to prepare imprinted microspheres was as follows: the template molecule (0.4 mmol) was mixed with the selected functional monomer (1.6 mmol) in a 15.0 mL screw-capped glass vial followed by addition of 10.0 mL THF as polymerization solvent. The cross-linker EGDMA (6 mmol) and the initiator AIBN (0.12 mmol) were then added to the above solution. To remove dissolved oxygen, the solution was purged with high purity nitrogen (99.999%) for 5 min. Finally, the test tube was sealed under the nitrogen atmosphere and was then placed in a water bath at 50 °C for 12 h with occasionally stirring. The resultant polymeric particles (1–3 μm) were collected and the template molecule was extracted from the polymers with 90/10 (v/v) MeOH/acetic acid mixture in a Soxhlet extraction system during 24 h. The reference non-imprinted polymers (NIPs) were prepared using the same procedure in the absence of template molecule.

2.6. Binding experiments

Polymer particles (100 mg) were added to 5.0 mL of polymerization solvent, i.e. THF, containing different concentrations of the drug and incubated for 12 h at room temperature. After the binding process was completed, the mixture was centrifuged and the concentration of free analyte was determined by HPLC. The amount of methocarbamol bound to the polymer (B) was calculated by subtracting the amount of free drug (F) from its initial value.

2.7. Molecularly imprinted solid phase extraction (MISPE)

2.7.1. MISPE-DPV

A 50 mg amount of each dry polymer was packed into empty 5 mL SPE-cartridges between two polyethylene frits. Prior to each extraction, cartridges were conditioned with 2.0 mL of phosphate buffer (1.0×10^{-3} mol L^{-1}, pH 7.0). To exactly 1.0 mL of human plasma, spiked with a known concentration of the drug, 0.6 g of ammonium sulfate was added and centrifuged at 7000 rpm for 15 min (4 °C) to precipitate proteins. The protein-free supernatant was diluted to 2.0 mL with phosphate buffer (pH 7.0) and then passed through the MIP or NIP cartridge. The cartridge was washed with 2× 0.5 mL of 95/5 (v/v) water/MeOH. The drug was eluted from the cartridge by using 2× 0.5 mL of 95/5 (v/v) MeOH/TFA. This fraction was then collected and concentrated up to dryness under a nitrogen stream. The sample was then reconstituted with 200 μL of methanol and diluted to 10 mL with 0.1 M phosphate buffer pH 3, and transferred to the voltammetric cell. The voltammogram was recorded as described in general procedure section.

2.7.2. MISPE-HPLC-UV

The procedure for MISPE-HPLC-UV was the same as MISPE-DPV except for the last step: after drying the sample, it was reconstituted with 200 μL of mobile phase of HPLC. A 20 μL volume of this solution was analyzed by HPLC.

2.8. Recovery experiments

A 50 mg amount of each dry polymer was packed into empty 5.0 mL SPE cartridges between two polyethylene frits. Prior to each extraction cartridges were conditioned with 2.0 mL of phosphate buffer (1.0×10^{-3} M, pH 7.0). A 1.0 mL solution of phosphate buffer (pH 7.0) spiked with a known concentration of methocarbamol was percolated through the MIP or NIP cartridge. The cartridges were then washed and eluted with corresponding washing or elution solvents. The elution fractions were then collected and peak area of methocarbamol was determined by HPLC. The extraction recoveries of methocarbamol during MISPE experiments were calculated using the formula:

$$\text{Recovery (MISPE)} = \left(\frac{A_{\text{Extracted}}}{A_{\text{Standard}}}\right) \times 100\% \quad (1)$$

where $A_{\text{Extracted}}$ is the peak area of methocarbamol in eluted fraction obtained by HPLC analysis after MISPE, and A_{Standard} is the peak area of methocarbamol standard in phosphate buffer without MISPE pretreating. A similar procedure was used to evaluate the recovery of analyte from a plasma sample after pretreating either by MISPE or C18-SPE cartridges.

The recovery of methocarbamol in spiked plasma samples using MISPE-HPLC-UV or MISPE-DPV methods was calculated using the formula:

$$\text{Recovery (method)} = \left(\frac{C_{\text{Found}}}{C_{\text{Spiked}}}\right) \times 100\% \quad (2)$$

where C_{Found} is the concentration of extracted methocarbamol by MISPE which obtained by HPLC or DPV techniques using calibration

curve, and C_{Spiked} is the concentration of initial methocarbamol in spiked plasma sample.

2.9. Clean-up procedure using C18-SPE cartridges

In order to compare MIP with classical reversed-phase SPE sorbents, a 5 mL-volume C18-SPE cartridge (Restek U.S., Bellefonte, PA) was used to extract the drug from a plasma sample. The SPE conditions were optimized and general procedure was as follows: the cartridge was preconditioned with 2.0 mL of methanol, followed by 2.0 mL of distilled water. To exactly 1.0 mL of human plasma, spiked with a known concentration of the drug, 0.6 g of ammonium sulfate was added and centrifuged at 5000 rpm for 15 min (4 °C) to precipitate proteins. The protein-free supernatant was diluted to 2.0 mL with phosphate buffer (pH 7.0) and then passed through the cartridge. The cartridge was washed with 2× 0.5 mL of 9/1 (v/v) water/MeCN and the drug was eluted with 2× 0.5 mL of 98/2 (v/v) of methanol/TFA solution. Elution fractions were collected in a test tube and evaporated to dryness under a nitrogen stream and dissolved in 200 μL of mobile phase of HPLC. A 20 μL volume of this solution was analyzed by HPLC.

2.10. Computational approach

All calculations have been carried out using Gaussian 03 [33] program. The computational method developed was based on the PM3 semiempirical method and density functional theory (DFT) to locate the most stable template–monomer complexes. The interaction energies, ΔE, were calculated through Eq. (3):

$$\Delta E = E(\text{template} - \text{monomer complex}) - E(\text{template}) - \sum E(\text{mononer}) \quad (3)$$

A well-known problem in the theory of intermolecular interactions is the occurrence of the so-called basis set superposition error (BSSE) [34]. As two molecules approach each other, the energy of the system falls not only because of the favorable intermolecular interactions but also because the basis functions on each molecule provide a better description of the electronic structure around the other molecule. Despite the well-known existence of BSSE and the means to correct it, only few reports of computationally assisted design of MIPs refer the correction of this error [24,35]. An approximate way of assessing BSSE is the counterpoise (CP) correction [36], which is widely used for the accurate computation of molecular interaction energies by *ab initio* and DFT methods [37,38].

Because polymerization is occurred in solution, we must take into account the effect of solvent, or solvation, in energy calculations because it leads to changes in energy and stability of the template–monomer complexes. Methods for evaluating the solvent effect may broadly be divided into two types: those describing the individual solvent molecules and those that treat the solvent as a continuous medium [39–41]. Continuum models [42], which are more popular, consider the solvent as a uniform polarizable medium with a dielectric constant of ε, while the solute is placed in a suitably shaped cavity in the medium [43]. In this section, the polarizable continuum model, developed by Tomasi and co workers [44–46], was used to study the effect of solvent in energy calculations.

In this study, electronic energies were first calculated using PM3 method. The most stable structures from this step were further optimized through the DFT method at B3LYP/6-31G(d,p) level. The BSSE error was corrected using the counterpoise (CP) correction. In order to introduce the effect of solvent in energy calculations, the polarizable continuum model was used.

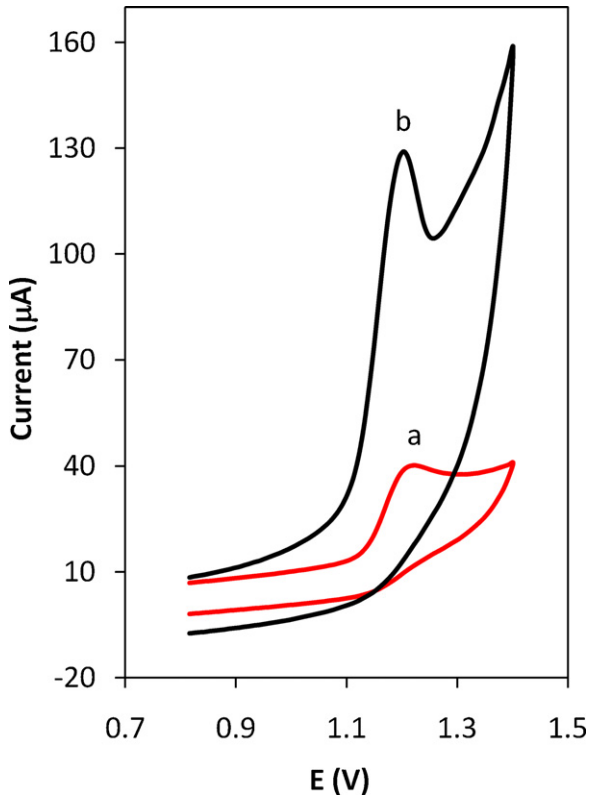

Fig. 1. Cyclic voltammograms of 1.0×10^{-5} mol L^{-1} methocarbamol in 0.1 mol L^{-1} phosphate buffer (pH 3) on: (a) GC and (b) GC/MWNT electrodes.

3. Results and discussion

3.1. Voltammetric study

Methocarbamol shows an irreversible oxidation wave in phosphate buffer solutions in the pH range 1.0–12.0. Fig. 1 shows the cyclic voltammetric response of the drug on a bare GC electrode (curve a) in phosphate buffer (pH = 3) within the potential window of 0.8–1.40 V. The anodic wave of methocarbamol is observed at the peak potential of 1.22 V. Curve b in Fig. 1 displays the cyclic voltammogram of the drug on a GC/MWNT electrode under the same experimental conditions. As can be seen, the Faradic response of methocarbamol at the GC/MWNT electrode is much higher than that observed at the bare GC electrode. The current enhancement for methocarbamol on modified GC electrode might be attributed to the large surface area of MWNT [47,48].

Cyclic voltammograms were also recorded at different potential scan rates from 10 to 500 mV s^{-1} on a GC/MWNT electrode. The linear relationship existing between peak current and square root of the scan rate showed that the oxidation process is predominantly diffusion-controlled in the whole scan rate range studied. The plots of logarithm of peak current versus logarithm of scan rate gave a straight line ($R^2 > 0.99$) with the slope of 0.55. This slope is close to the theoretically expected value of 0.50 for a diffusive process [49]. On the other hand, as scan rate increased, the potential shifted to more positive values as expected for an irreversible oxidation process [50]. The plot of E_p vs. log υ resulted in a straight line ($r^2 > 0.99$) with a slope of 59.3 mV/decade ($30/\alpha n_a$) [51]. Therefore αn_a value was found to be 0.5. Since the value of α is normally considered to be 0.5, the number of electrons, n_a transferred in the rate-determining step should be one ($n_a = 1$).

Similar experiments were carried out by differential pulse voltammetry. Fig. 2 shows the DPVs of methocarbamol in phos-

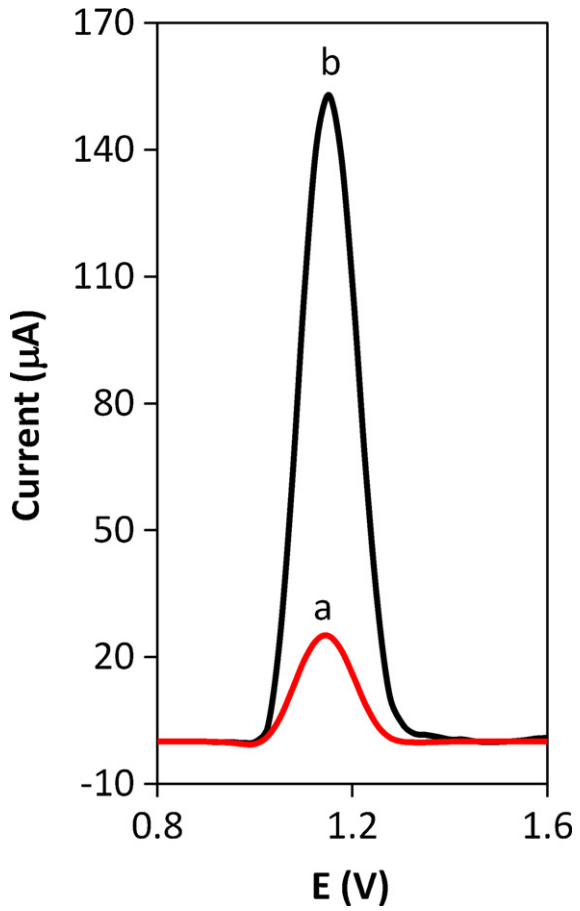

Fig. 2. Differential pulse voltammograms of 1.0×10^{-7} mol L^{-1} methocarbamol in 0.1 mol L^{-1} phosphate buffer (pH 3) on: (a) GC and (b) GC/MWNT electrodes.

phate buffer (pH 3) at the bare GC (curve a) and GC/MWNT (curve b) electrodes, respectively. The DPV of 1×10^{-7} M of methocarbamol at GC/MWNT electrode shows an about 6-fold increase in anodic current relative to that obtained by the bare GC electrode. Therefore, the DPV mode using the GC/MWNT as working electrode was selected for quantitative analysis of the drug.

The electrochemical oxidation of methocarbamol at the GC/MWNT electrode was investigated in the pH range 1.0–12.0. The relationship between the peak height and pH for the oxidation process of methocarbamol is shown in Fig. 3. The peak height was

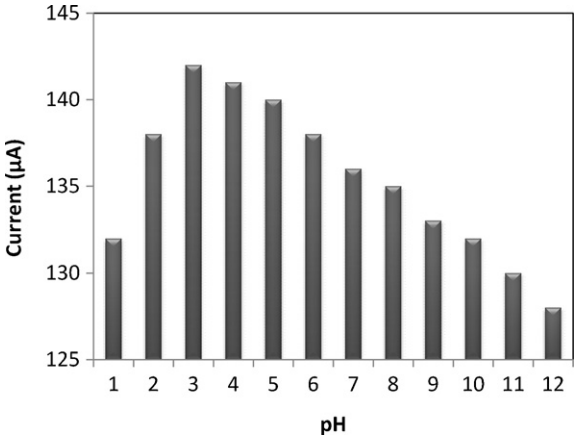

Fig. 3. Effect of pH on the peak currents of differential pulse voltammograms of 1×10^{-7} mol L^{-1} methocarbamol.

Table 1
Calculated interaction energies (kJ/mol) for the most stable 13 template–monomer complexes at B3LYP/6-31G(d,p) level in the gas phase with and without BSSE correction.

Monomer	$\Delta E_{\text{non-corr}}$	ΔE_{corr}
AA	−167.6925	−121.951
MAA	−165.3164	−120.105
HEMMA	−120.1675	−78.5824
ALAM	−79.88790	−23.1899

pH dependent and the maximum peak current value was obtained at pH 3.0, hence this pH was chosen to carry out electroanalytical determinations.

The electrochemical oxidation of methocarbamol seems to be a complex process and different reaction pathways are possible. From the voltammetric behavior of alkoxybenzene derivatives, which are structurally related to methocarbamol [52,53], the mechanism of oxidation of methocarbamol may be postulated by oxidation of the –OMe and/or –OR ($R = CH_2CH_2OHCH_2OCONH_2$) groups on the aromatic ring (Scheme 2) [54–56].

The influence of electrochemical parameters known to affect the differential pulse voltammograms viz. pulse amplitude, pulse width and scan rate were studied. The variables of interest were studied over the ranges 10–200 mV for pulse amplitude, 100–2000 ms for pulse width and 10–250 mV s^{-1} for scan rate. To acquire a well shape voltammogram with high peak current, the values of 100 mV, 250 ms and 100 mV s^{-1} were chosen for pulse amplitude, pulse width and scan rate, respectively.

3.2. Theoretical selection of functional monomer and polymerization solvent

The selection of suitable functional monomers for imprinting process may be aided by molecular modeling and computational methods [57]. In a typical computational approach, a virtual library of functional monomers is created and screened for all possible interactions between monomers and the template molecule. Monomers with the highest binding scores are subsequently selected to produce full scale MIPs with hopefully superior recognition properties. In this work, eighteen functional monomers (Scheme 3) were theoretically selected as possible functional monomers. The conformation of template, functional monomers and template–monomer complexes were first optimized to the lowest energy using the fast PM3-semiempirical method. In the calculation of electronic energies, the highest stability was obtained for the 1:3 mole ratio of template–monomer complexes. Among the monomers tested, MAA, AA and HEMMA gave the most stable complexes with the template molecule, while the lowest binding energy was obtained with ALAM. These structures were further optimized using a more accurate quantum mechanical calculation. Fig. 4, as an example, shows the optimized geometries of 1:1, 1:2 and 1:3 methocarbamol–AA complexes predicted by DFT method at B3LYP/6-31G(d,p) level. Table 1 summarizes the calculated interaction energies for 1:3 template–monomer complexes before and after BSSE correction in the gas-phase. As seen, DFT predicts that the most stable complex is formed between AA and template molecule. The CP correction also reveals that the values of binding energies are influenced by BSSE but the stability order is maintained. The interaction energies were also calculated in different solvents using the cosmo polarizable continuum model. The interaction energies obtained with different implicit solvents corresponds in every case to a significant decrease as compared to the gas-phase interaction. This makes sense since solvation of a species involves also intermolecular interactions of the same nature as monomer–template and so the solvent acts as a competitor. From the data listed in

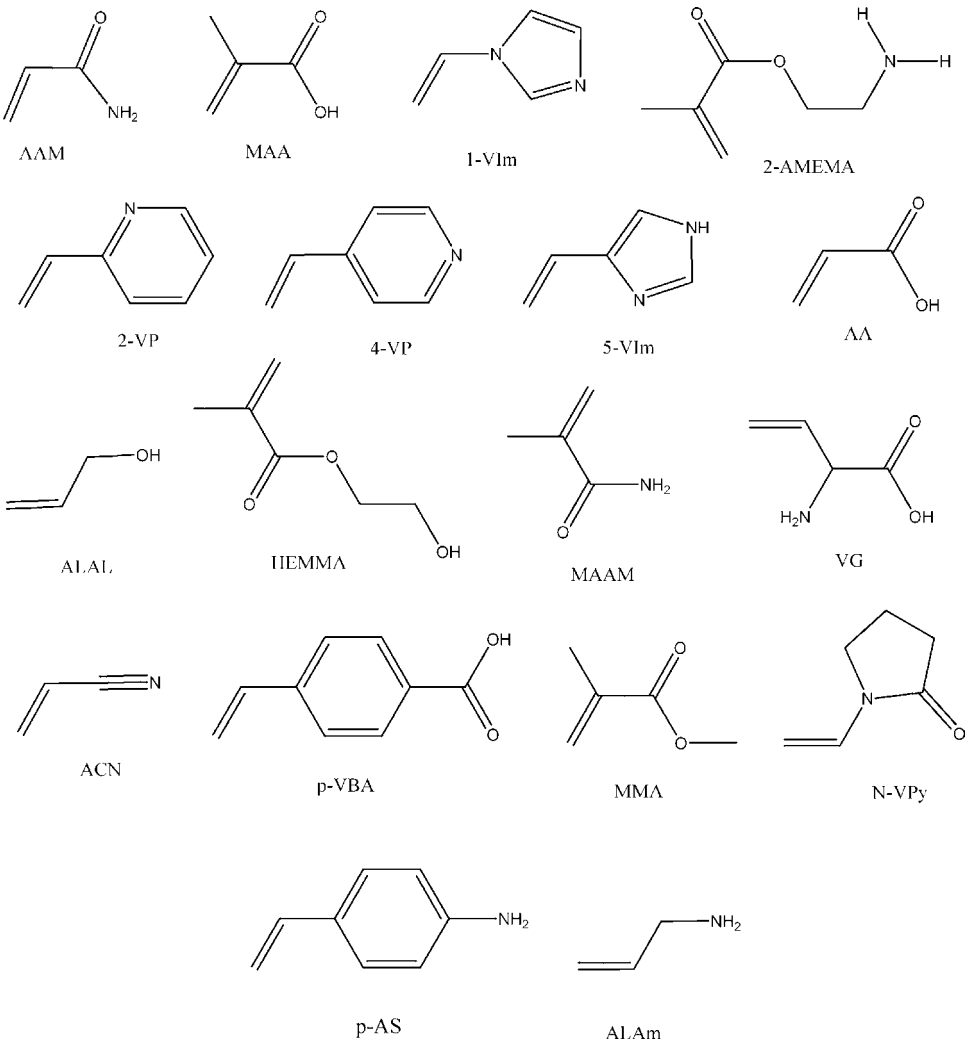

Scheme 3. The virtual library of functional monomers: acrylamide (AAM), methacrylic acid (MAA), 1-vinylimidazole (1-Vlm), 2-aminoethylmethacrylate (2-AMEMA), 2-vinylpyridine (2-VP), 4-vinilpyridine (4-VP), 1-vinylimidazole (1-Vim), acrylic acid (AA), allyl alcohol (ALAL), hydroxyethyl methacrylate (HEMMA), methacrylamide (MAAM), vinylglycine (VG), acrylonitrile (ACN), p-vinylbenzoic acid (p-VBA), methyl methacrylate (MMA), N-vinylpyrroline (N-Vpy), p-aminostyrene (p-AS) and allylamine (ALAM).

Table 2, it is concluded that THF is the most favorable solvent for preparation of MIP.

3.3. Adsorption isotherm

Three molecularly imprinted polymers were prepared with AA (MIP1), HEMMA (MIP2) and ALAM (MIP3) for adsorption studies. The heterogeneous Langmuir–Freundlich (LF) isotherm was considered for evaluation of binding characteristics of the synthesized MIPs [58]. The LF isotherm describes a relationship between the concentration of bound (B) and free (F) guest in heterogeneous systems with three different coefficients according to the following equation:

$$B = \frac{N_t a F^m}{1 + aF^m} \quad (4)$$

where N_t is the total number of binding sites, a is related to the median binding affinity constant (K_0) via ($K_0 = a^{1/m}$), and m is the heterogeneity index, which will be equal to 1 for a homogeneous material, or will take values within 0 and 1 if the material is heterogeneous. The experimental isotherm data (F and B) were successfully fitted to the LF isotherm in order to evaluate the N_t, K_0, and m values. The resulted fitting coefficients at the desired concentration window are listed in Table 3. As seen,

Table 2
Calculated interaction energies (kJ/mol) for the most stable 13 template–monomer complexes at B3LYP/6-31G(d,p) level different solvents using CPCM model.

Monomer	Solvent				
	Water	DMSO	Acetonitrile	Acetone	THF
AA	−63.684	−62.523	−64.025	−69.084	−79.505
MAA	−62.833	−61.150	−62.589	−64.373	−73.322
HEMMA	−39.884	−34.121	−37.840	−38.890	−40.340
ALAM	7.6747	16.336	13.259	12.335	7.2932

Table 3
Langmuir–Freundlich isotherm fitting coefficients for MIP1 and MIP2.

Polymer	Isotherm parameters				R^2
	N_t (μmol g^{-1})	a (g μmol^{-1})	m	K_0[a] (g μmol^{-1})	
MIP1	478.6	0.031	0.58	0.0025	0.997
MIP2	355.5	0.016	0.53	0.0004	0.998
MIP3	98.60	0.019	0.50	0.0004	0.993

[a] The mean association constant which was calculated as $K_0 = a^{1/m}$.

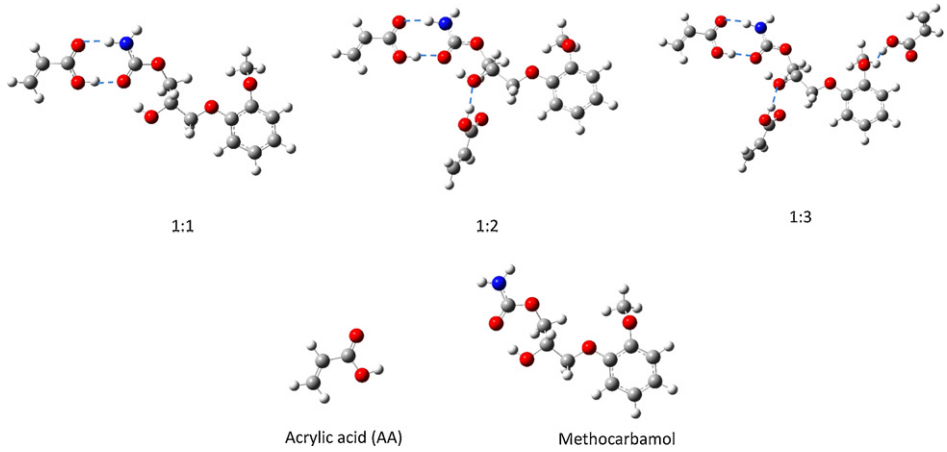

Fig. 4. Computationally derived structures of 1:1, 1:2 and 1:3 complexes of methocarbamol with AA using DFT method at B3LYP/6-31G(d,p) level.

the value of m demonstrates the heterogeneity of all MIPs. However, MIP1 shows a better degree of binding site homogeneity ($m = 0.58$), a higher concentration of binding sites per gram of polymer ($N_t = 478.6\ \mu mol\ g^{-1}$) and a grater median binding affinity ($K_0 = 2.5 \times 10^{-3}\ \mu mol^{-1}$).

3.4. Optimization of MISPE procedure

3.4.1. Effect of pH

To have a better interaction between MIP and target molecule in aqueous media, the effect of sample pH should be studied. The effect of buffer pH on methocarbamol binding was investigated over the pH range 2.0–12.0 (Fig. 5). Clearly, the binding of methocarbamol was not greatly affected at pHs < 8.0. However, at more alkaline pHs the recovery of the drug was decreased as pH increased. It is reported that methocarbamol is unstable at alkaline media [59] which may be the main reason of decreasing recovery at higher pHs. The pH 7.0 was selected for subsequent MISPE experiments.

3.4.2. Selection of washing solvent

Washing MIP is a crucial step in developing a MISPE procedure because the general procedure for reducing problems of nonspecific adsorption is the selection of a proper washing solvent prior to elution [60]. Thus, in this section several washing solvents/solutions were tested to develop a proper washing step (Table 4). Solvents such as water, methanol and acetonitrile and their binary mixtures were tested. It was found that higher ratios of organic solvent in washing solution yielded chromatograms with less contaminant peaks and the best results were obtained when methanol was used. With increasing percentage of methanol, however, analyte recovery decreased. However, addition of up to 5% methanol to water could be permitted without considerable loss of recovery. The final MISPE procedure uses an aqueous wash with 2× 0.5 mL of water–methanol (95:5, v/v) with loss of analyte being less than 3.5%. This composition of water and methanol also serves the maximum difference between MIP and NIP's recovery. Other washing solutions such as water/acetic acid, water/TFA and water/TEA gave poor recovery.

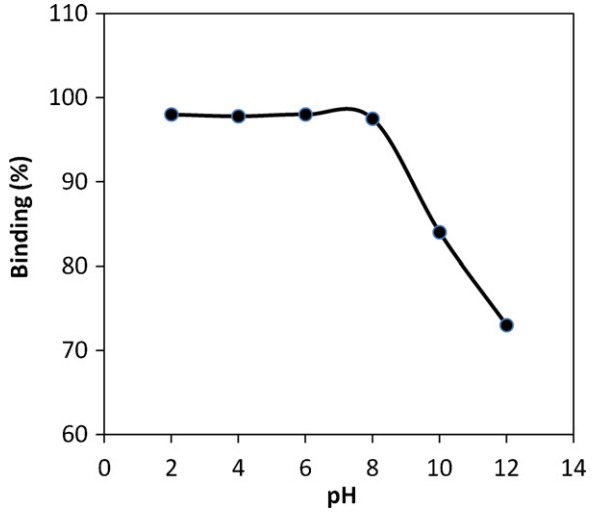

Fig. 5. Effect of pH on the adsorption of methocarbamol onto MIP1.

3.4.3. Selection of elution solvent

The strong imprint–analyte interaction must be destroyed to reach a high extraction recovery; therefore a series of experiments was performed to study the elution solvent composition. Solvents such as methanol, acetonitrile and THF were tested as eluents. Among these solvents the best recoveries were obtained using MeOH (Table 5). Addition of small amounts of TFA up to 5% in MeOH also increased elution strength. Higher amounts of TFA in MeOH, however, had no significant effect on recoveries. Therefore, 2× 0.5 mL of 95/5 (v/v) MeOH/TFA was used as elution solution throughout the study.

3.5. The selectivity test

To evaluate the selectivity of the synthesized MIP, mephenesin and guaifenesin two structural analogue of methocarbamol, and several drugs with different structures were considered in this section (Scheme 1). In several batch experiments, the distribution ratio

Table 4
Methocarbamol recoveries (%) from MIP and NIP cartridges after washing with 2× 0.5 mL of different washing solvents/solutions.

Washing solvent	MIP	NIP	Difference
Acetonitrile	25.4	0.0	25.4
MeOH	22.5	0.0	22.5
Water	99.7	46.6	53.1
Water/MeOH (98/2)	97.6	4.1	93.5
Water/MeOH (95/5)	96.5	<0.5	96.0
Water/MeOH (90/10)	93.7	<0.1	93.6
Water/TFA (98/2)	67.5	2.7	64.8
Water/TEA (98/2)	69.8	3.0	66.8
Water/acetic acid (98/2)	72.3	3.6	68.7

Table 5
Typical recovery of methocarbamol from MIP cartridge using different elution solvents/solutions.[a]

Eluent	First (%)	Second (%)	Third (%)	Fourth (%)	Total recovery (%)
Acetonitrile	53.5	30.9	4.6	1.0	90.0
MeOH	55.8	32.3	6.5	1.2	95.8
THF	52.0	31.4	4.4	<0.2	88.0
MeOH/TFA (98/2)	68.5	27.4	0.4	0.0	96.3
MeOH/TFA (95/5)	70.3	26.5	<0.1	0.0	96.9

[a] The volume of eluent in each step was 0.5 mL.

(K_d) and selectivity coefficients (α) were calculated. The K_d values were calculated using the equation:

$$K_d = \frac{(C_i - C_f)V}{C_f m} \quad (5)$$

where V, C_i, C_f and m represent the volume of the solution (mL), drug concentration before and after adsorption ($\mu g\,mL^{-1}$) and mass of the polymer, respectively. The selectivity coefficient (α) is defined as:

$$\alpha = \frac{K_d \ (\text{Methocarbamol})}{K_d \ (\text{Foreign compound})} \quad (6)$$

Table 6 summarizes the K_d and α values of tested drugs when MIP and NIP were used. The selectivity coefficient is an indicator to express an adsorption affinity of recognition sites for each drug. The α values greater than 2 indicate that the unique shape of the template molecule plays an important role in its selective binding to the MIP.

3.6. Validation of MISPE-DPV and MISPE-HPLC-UV methods

3.6.1. MISPE-DPV

The MISPE-DPV method for the determination of methocarbamol was validated by determining its performance characteristics regarding linearity, sensitivity and precision. The standard calibration curve of MISPE-DPV for methocarbamol determination in human plasma was linear over the range 0.10–15.0 $\mu g\,mL^{-1}$ ($n = 15$). The relationship between peak height (y, μA) and concentration (x, $\mu g\,mL^{-1}$) could be expressed by the equation $y = 4.611x - 0.455$; ($R^2 = 0.996$). As defined by European Pharmacopoeia [61], the LOQ and LOD are the concentrations at which the signal to noise ratio is 3 and 10, respectively. The limit of detection (LOD) and the limit of quantification (LOQ) were 0.025 and 0.05 $\mu g\,mL^{-1}$, respectively. The RSD value of 0.5 $\mu g\,mL^{-1}$ solution of drug ($n = 6$) was found to be 1.86% indicating good repeatability of the method.

3.6.2. MISPE-HPLC-UV

The analysis of methocarbamol was also carried out by high performance liquid chromatography. The peak corresponding to methocarbamol has a retention time of 6.0 min in a mobile phase composed of acetonitrile and phosphate buffer (pH = 3) (50/50, v/v) at a flow rate of 1.0 mL min^{-1}. The calibration curve was obtained by plotting peak area values of methocarbamol standards in plasma against the methocarbamol concentrations. Linearity was observed between 0.5 and 18.0 $\mu g\,mL^{-1}$ of methocarbamol concentrations. The equation of the calibration line, obtained by the least-square regression was: $y = 132.18x + 4185$; ($R^2 = 0.997$), ($n = 15$) where x is the methocarbamol concentration, expressed as $\mu g\,ml^{-1}$, and y is the peak area value of methocarbamol. The LOD and LOQ values were 0.065 $\mu g\,mL^{-1}$ and 0.125 $\mu g\,mL^{-1}$, respectively, calculated according to European Pharmacopoeia [57]. The intraday precision assays gave RSD values of 1.74% for repeatability on 0.5 $\mu g\,mL^{-1}$ methocarbamol standard solution ($n = 6$).

Table 6
Distribution ratio (K_d) and selectivity coefficient (α) values for imprinted and non-imprinted polymers.

Compound	MIP		NIP	
	K_d	α	K_d	α
Methocarbamol	358.7		37.4	
Mephenesin	166.9	2.14	38.9	0.96
Guaifenesin	153.8	2.33	37.7	0.99
Acetazolamide	75.9	2.88	28.0	1.33
Metronidazole	48.8	7.35	22.5	0.49
Zonisamide	45.9	7.81	18.9	1.97

3.7. MISPE versus C18-SPE cartridges

To compare the performance of the proposed MISPE procedure with commercial SPE sorbents, chromatograms were recorded after

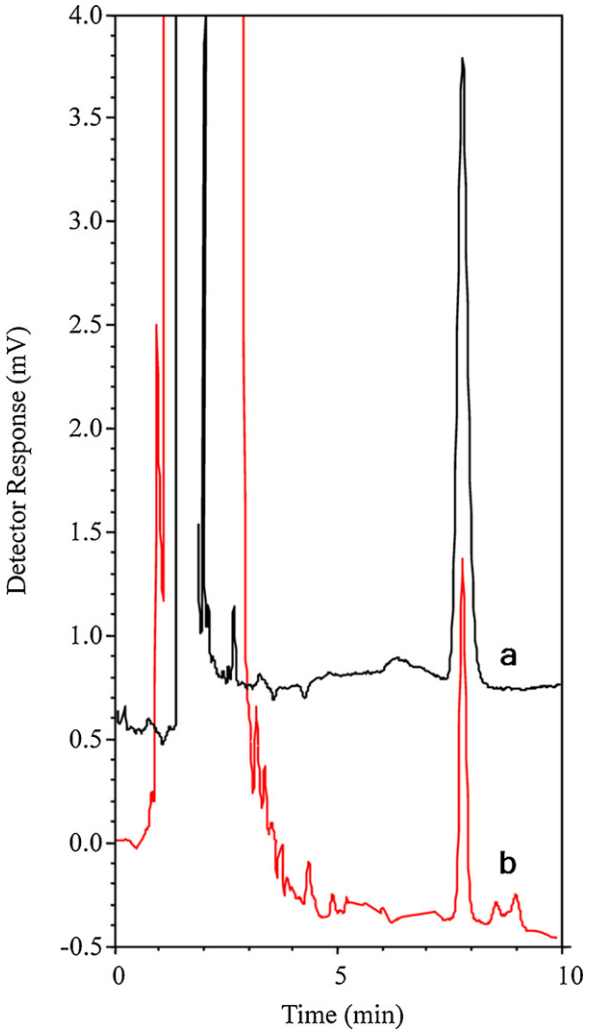

Fig. 6. HPLC chromatograms of a plasma sample spiked with methocarbamol (0.5 $\mu g\,mL^{-1}$) after clean-up with (a) MIP and (b) C18-cartridge.

Table 7
Results of determination of methocarbamol in human plasma ($n = 5$).

Concentration ($\mu g\,ml^{-1}$)	MISPE-DPV ($\mu g\,ml^{-1}$)	Recovery (%)	MISPE-HPLC-UV ($\mu g\,ml^{-1}$)	Recovery (%)	t-Test[a]	f-Test
0.5	0.47 ± 0.017	94.0	0.48 ± 0.012	96.0	0.69	2.04
1.0	0.97 ± 0.025	97.0	0.97 ± 0.019	97.0	0.10	1.69
2.5	2.45 ± 0.064	98.0	2.44 ± 0.055	97.6	0.35	1.32

[a] Theoretical values of t and f at $P = 0.05$ are 2.31 and 6.39, respectively.

extraction of methocarbamol from human plasma using both C18 and MIP cartridges. Results are shown in Fig. 6. On a C18-cartridge the recovery of the drug was less than 59.0% compared with 91.8% for MIP cartridge (Eq. (1)). The enhancement of selectivity brought by the MIP for the treatment of a complex matrix is clearly demonstrated. The chromatogram resulting from the MISPE shows a cleaner baseline than the one obtained for the C18-cartridge. Also, it is worth noting that a cartridge packed with 50 mg of MIP can be used for clean-up of at least 15 plasma samples with no noticeable deterioration in performance while C18-cartridges lose their performance after one or two extractions. The MISPE cartridge can be regenerated by washing with 2 mL MeOH/acetic acid (9/1, v/v) and 2 mL water.

3.8. Analysis of human plasma samples

The applicability of both MISPE-DPV and MISPE-HPLC-UV methods was tested for human plasma samples. Table 7 compares the results of the analysis of methocarbamol between the two methods. The results were compared by Student's t-test and f(fisher)-test and there was no significant difference between accuracy and precision of the proposed methods.

4. Conclusion

In conclusion, the results presented here demonstrate the usefulness of computational methods for rapid screening of functional monomers for a specified template molecule in an experiment-free way. Rapid selection of functional monomers could be achieved by combination of semiempirical and quantum mechanical calculations. According to the theoretical calculations, AA and THF were selected as functional monomer and polymerization solvent, respectively. The MIP with methocarbamol as template was prepared by precipitation polymerization method. The new sorbent revealed a good selectivity toward the template molecule over other structurally related compounds. The high extraction recovery, high selectivity and high physical and chemical robustness of the synthesized MIP enabled its applicability as a good sorbent for molecularly imprinted solid-phase extraction applications.

References

[1] E.B. Carpenter, South. Med. J. 51 (1958) 627.
[2] United States Pharmacopeia XXII, United States Pharmacopeial Convention, Rockville, MD, 1990.
[3] R.B. Bruce, L.B. Turnbull, J.H. Newman, J. Pharm. Sci. 60 (1971) 104.
[4] M. Kemal, R. Imami, A. Poklis, J. Forensic Sci. 27 (1982) 217.
[5] A.A. Forist, R.W. Judy, J. Pharm. Sci. 60 (1971) 1686.
[6] K.E. Ferslew, A.N. Hagardorn, W.F. McCormick, J. Forensic Sci. 35 (1990) 477.
[7] W. Zha, Z. Zhu, J. Chromatogr. B 878 (2010) 831.
[8] N. Erk, Y. Özkan, E. Banoğlu, S.A. Özkan, Z. Şentürk, J. Pharm. Biomed. Anal. 24 (2001) 469–475.
[9] W. Naidong, J.W. Lee, J.D. Hulse, J. Chromatogr. B 654 (1994) 287.
[10] N. Jiang, Electroanalytical Chemistry Research Developments, Nova Publishers, New York, 2007.
[11] L. Chimuka, M. van Pinxteren, J. Billing, E. Yilmaz, J. Åke Jönsson, J. Chromatogr. A 1218 (2011) 647.
[12] G. Zhu, J. Fan, Y. Gao, X. Gao, J. Wang, Talanta 84 (2011) 1124.
[13] C. Zhao, T. Zhao, X. Liu, H. Zhang, J. Chromatogr. A 1217 (2010) 6995.
[14] Y. Li, W.H. Zhou, H.H. Yang, X.R. Wang, Talanta 79 (2009) 141.
[15] H. Yan, K.H. Row, G. Yang, Talanta 75 (2008) 227.
[16] B. Sellergren, L.I. Andersson, Methods 22 (2000) 92.
[17] K. Ensing, T. de Boer, Trends Anal. Chem. 18 (1999) 138.
[18] L.I. Andersson, J. Chromatogr. B 739 (2000) 163.
[19] D. Stevenson, Trends Anal. Chem. 18 (1999) 154.
[20] Y. Li, X. Li, Y. Li, C. Dong, P. Jin, J. Qi, Biomaterials 30 (2009) 3205.
[21] J. Yao, X. Li, W. Qin, Anal. Chim. Acta 610 (2008) 282.
[22] M. Azenha, P. Kathirvel, P. Nogueira, A. Fernando-Silva, Biosens. Bioelectron. 23 (2008) 1843.
[23] I.A. Nicholls, H.S. Andersson, C. Charlton, H. Henschel, B.C.G. Karlsson, J.G. Karlsson, J. O'Mahony, A.M. Rosengren, K.J. Rosengren, S. Wikman, Biosens. Bioelectron. 25 (2009) 543.
[24] M.B. Gholivand, M. Khodadadian, F. Ahmadi, Anal. Chim. Acta 658 (2010) 225.
[25] M. Khodadadiana, F. Ahmadi, Talanta 81 (2010) 1446.
[26] A. Merkoci, Microchim. Acta 152 (2006) 157.
[27] M. Valcarcel, B.M. Simonet, S. Cardenas, B. Suarez, Anal. Bioanal. Chem. 382 (2005) 1783.
[28] J.J. Gooding, Electrochim. Acta 50 (2005) 3049.
[29] A. Merkoci, M. Pumera, X. Llopis, B. Perez, M. del Valle, S. Alegret, Trends Anal. Chem. 24 (2005) 826.
[30] Y. Zhou, H. Yang, H.Y. Chen, Talanta 76 (2008) 419.
[31] S.E. Kooi, U. Schlecht, M. Burghard, K. Kern, Angew. Chem. Int. Ed. 41 (2002) 1353.
[32] K. Jurkschat, X. Ji, A. Crossley, R.G. Compton, C.E. Banks, Analyst 132 (2007) 21.
[33] M.J. Frisch, G.W. Trucks, H.B. Schlegel, G.E. Scuseria, M.A. Robb, J.R. Cheeseman, V.G. Zakrzewski, J.J.A. Montgomery, R.E. Stratmann, J.C. Burant, S. Dapprich, J.M. Millam, A.D. Daniels, K.N. Kudin, M.C. Strain, O. Farkas, J. Tomasi, V. Barone, M. Cossi, R. Cammi, B. Mennucci, C. Pomelli, C. Adamo, S. Clifford, J. Ochterski, G.A. Petersson, P.Y. Ayala, Q. Cui, K. Morokuma, D.K. Malick, A.D. Rabuck, K. Raghavachari, J.B. Foresman, J. Cioslowski, J.V. Ortiz, B.B. Stefanov, G. Liu, A. Liashenko, P. Piskorz, I. Komaromi, R. Gomperts, R.L. Martin, D.J. Fox, T. Keith, M.A. Al-Laham, C.Y. Peng, A. Nanayakkara, C. Gonzalez, M. Challacombe, P.M.W. Gill, B. Johnson, W. Chen, M.W. Wong, J.L. Andres, C. Gonzalez, M. Head-Gordon, E.S. Replogle, J.A. Pople, Gaussian 03, Revision C.01, Gaussian Inc., Pittsburgh, PA, 2003.
[34] B. Liu, A.D. McLean, J. Chem. Phys. 59 (1973) 4557.
[35] N. Mukawa, T. Goto, H. Nariai, Y. Aoki, A. Imamura, T. Takeuchi, J. Pharm. Biomed. Anal. 30 (2003) 1943.
[36] J.C. Slater, The Self-Consistent Field for Molecules and Solids: Quantum Theory of Molecules and Solids, vol. 4, McGraw-Hill, New York, 1974.
[37] C.J. Cramer, Essentials of Computational Chemistry: Theories and Models, second ed., John Wiley & Sons, Inc., Chichester, England, 2004.
[38] J. Frank, Introduction to Computational Chemistry, second ed., John Wiley & Sons, Inc., Chichester, England, 2007.
[39] K.V. Mikkelsen, H. Ågren, J. Mol. Struct. (Theochem.) 234 (1991) 425.
[40] C.J. Cramer, D.G. Truhlar, Chem. Rev. 99 (1999) 2161.
[41] P.E. Smith, B.M. Pettitt, J. Phys. Chem. 98 (1994) 9700.
[42] B. Roux, T. Simonson, Biophys. Chem. 78 (1999) 1.
[43] M. Cossi, V. Barone, R. Cammi, J. Tomasi, Chem. Phys. Lett. 255 (1996) 327.
[44] J. Tomasi, M. Persico, Chem. Rev. 94 (1994) 2027.
[45] S. Miertus, G. Scrocco, J. Tomasi, Chem. Phys. 55 (1981) 117.
[46] S. Miertus, J. Tomasi, Chem. Phys. 65 (1982) 239.
[47] X. Lin, Y. Li, Biosens. Bioelectron. 22 (2006) 253.
[48] T.L. Lu, Y.C. Tsai, Sens. Actuators B: Chem. 148 (2010) 590.
[49] D.K. Gosser, Cyclic Voltammetry: Simulation and Analysis of Reaction Mechanisms, VSH, New York, 1993.
[50] A.M. Bond, Modern Polarographic Methods in Analytical Chemistry, Dekker (Marcel), New York, 1980.
[51] E. Hammam, A. Tawfik, M.M. Ghoneim, J. Pharm. Biomed. Anal. 36 (2004) 149.
[52] C.C. Zeng, J.Y. Becker, J. Org. Chem. 69 (2004) 1053.
[53] N.L. Weinberg, B. Belleau, Tetrahedron 29 (1973) 279.
[54] B. Fabre, K. Michelet, N. Simonet, J. Simonet, J. Electroanal. Chem. 425 (1997) 67.
[55] V. Le Berre, L. Angely, J. Simonet, J. Electroanal. Chem. 218 (1987) 173.
[56] D.R. Henton, R.L. McCreery, J.S. Swenton, J. Org. Chem. 45 (1980) 369.
[57] S.A. Piletsky, K. Karim, E.V. Piletska, C.J. Day, D.W. Freebairn, C. Legge, A.P.F. Turner, Analyst 126 (2001) 1826.
[58] R.J. Umpleby, S.C. Baxter, Y. Chen, R.N. Shah, K.D. Shimizu, Anal. Chem. 73 (2001) 4584.
[59] N. Pouli, A.A. Vyzas, G.B. Foscolos, J. Pharm. Sci. 83 (1994) 499.
[60] S. Piletsky, A. Turner, Molecular Imprinting of Polymers, Landes Bioscience, Texas, USA, 2006.
[61] European Pharmacopoeia, fourth ed., European Department for the Quality of Medicines, Strasbourg, France, 2002.